



# Fuel Sorption into Polymers : Experimental and Machine Learning Studies

Benoit Creton, Benjamin Veyrat, Marie-Hélène Klopffer

## ► To cite this version:

Benoit Creton, Benjamin Veyrat, Marie-Hélène Klopffer. Fuel Sorption into Polymers : Experimental and Machine Learning Studies. Fluid Phase Equilibria, 2022, 556, pp.113403. 10.1016/j.fluid.2022.113403 . hal-03585804

**HAL Id: hal-03585804**

**<https://ifp.hal.science/hal-03585804>**

Submitted on 23 Feb 2022

**HAL** is a multi-disciplinary open access archive for the deposit and dissemination of scientific research documents, whether they are published or not. The documents may come from teaching and research institutions in France or abroad, or from public or private research centers.

L'archive ouverte pluridisciplinaire **HAL**, est destinée au dépôt et à la diffusion de documents scientifiques de niveau recherche, publiés ou non, émanant des établissements d'enseignement et de recherche français ou étrangers, des laboratoires publics ou privés.

# Fuel sorption into polymers: experimental and machine learning studies.

Benoit Creton\*, Benjamin Veyrat, Marie-Hélène Klopffer

*IFP Energies nouvelles, 1 et 4 avenue de Bois-Préau, 92852 Reuil-Malmaison, France.*

---

## Abstract

In the automotive industry, the introduction of alternative fuels in the market or even the consideration of new fluids such as lubricants requires continuous efforts in research and development to predict and evaluate impacts on materials (e.g., polymers) in contact with these fluids. We address here the compatibility between polymers and fluids by means of both experimental and modelling techniques. Three polymers were considered: a nitrile butadiene rubber (NBR), a fluorinated elastomer (FKM) and a fluorosilicon rubber (FVMQ), and a series of hydrocarbons mixtures were formulated to study the swelling of the polymers. The swelling of samples has been investigated in terms of weight and not volume variations as the measure of this former is assumed to be more accurate. Multi-gene genetic programming (MGGP) was applied to experimental data obtained in order to derive models to predict: (i) the maximum value of the mass gain ( $\Delta M$ ) and (ii) the sorption kinetics, *i.e.* the time evolution of  $\Delta M$ . Predicted values are in excellent agreement with experimental data (with  $R^2$  greater than 0.99), and models have demonstrated their predictive capabilities when applied to external fluids (not considered during the training procedure). Combining experiments and modelling, as proposed in this work, leads to accurate models which drastically reduce the time necessary to quantify polymeric materials compatibility with a fluid candidates as compared to experiments.

**Keywords:** Polymer, Fuels, Machine Learning, Sorption

---

---

\*Corresponding author: benoit.creton@ifpen.fr

## 1. Introduction

In the context of global warming, conclusions of research dedicated to the reduction of greenhouse gases emissions advocate the use of alternative fuels [1]. In particular, advanced fuels and biofuels including conventional renewable fuels, respecting environmental criteria at a reasonable cost are of primary interest [2]. Biofuels are issued from organic raw materials and they can be seen as blends of renewable molecules such as normal- and iso-paraffins, naphthenic and aromatic compounds, normal- and iso-olefins, alcohols, and/or esters [3]. Normal- and iso-paraffins can be obtained by industrial processes such as Fisher-Tropsch (FT) [4] and hydrotreatment of vegetable oils (HVO) [5]. In the same way, naphthenic and aromatic compounds can be synthesized from the liquefaction or pyrolysis of biomass [6, 7]. Moreover, compositions constantly evolving and being different from one country to another, it has become essential to understand the impact of the introduction of these compounds on the physical properties of alternative fuels. The presence of these families of molecules with different chemistry requires extensive research and development activities. Indeed, it drives the conditions for storage, transportation, and combustion quality.

In combustion engine vehicles many pieces of the fuel-delivery systems are composed all or part of polymers. Polymeric materials in contact with fuels and/or biofuels may be subject to deformations such as swelling, caused by solvent ingress within their structure and leading to strong modifications and loss of their initial physical and chemical properties [8, 9]. To address this problem, one solution consists in using multilayer structures containing interleaved barrier polymers [10]. Up to date, only few works have been published in the literature dealing with the compatibility between polymeric materials and fluids, and there is a lack of available experimental data [11]. The group of Izák *et al.* have investigated experimentally and theoretically gases and liquids sorption into polymers over the last decades [12, 13, 14] ; and more recently, Krajakova *et al.* focused on sorption of liquids into poly(ethylene) samples of different densities [15]. Regarding fuels, Haseeb *et al.* immersed some elastomeric materials such as nitrile butadiene rubber (NBR) and Viton® a fluorinated elastomer (FKM) in diesel and palm biodiesel to compare the degradation of physical properties like weight and volume changes, hardness and tensile strength [16, 17]. Kaas *et al.* studied the compatibility of elastomeric materials with gasoline blends containing ethanol and isobutanol, followed evolution of some polymer's properties, and

38 proposed a ranking of elastomer specimens according to their swelling [18].  
 39 Silva *et al.* ordered some rubbers as a function of their compatibility with  
 40 biodiesels, and revealed that the mobility of chains of NBR in biodiesel in-  
 41 creases without change in their chemical structures [19]. In the article by  
 42 Trakarnpruk *et al.*, authors studied elastomer properties after immersion  
 43 in biodiesel, focusing among others on NBR, copolymers, and terpolymer  
 44 FKM. Authors concluded that among tested polymers fluoroelastomers un-  
 45 dergo fewer physical degradation [20]. Weltshev *et al.* focused their research  
 46 on the resistance of sealing materials such as FKM, NBR and fluorosilicon  
 47 rubber (FVMQ), immersed during hours in biodiesel based fuels, as a func-  
 48 tion of the age and the temperature of fluids [21]. Authors noted that the  
 49 percentage of degradation is proportional to the temperature and the age  
 50 of the fuels. In regards to available experimental results, it appears that  
 51 current methods used for the data acquisitions are time consuming, and the  
 52 development of robust predictive models is of high relevance.

53 Plota and Masek recently reviewed kinetic based models used to predict  
 54 the lifetime of polymeric materials and conclude to the necessity of develop-  
 55 ing new methods [22]. During last decades materials informatics has emerged  
 56 as a new approach for the conception of new materials [23, 24, 25]. It consists  
 57 in training learning algorithms on database content, in order to allow pre-  
 58 dictions for materials having structures similar to those contained within the  
 59 database, or even to propose promizing candidates for specific applications.  
 60 Polymer informatics necessitates relevant databases which integrate knowl-  
 61 edge about properties related to thermodynamics, mechanics, optics, and  
 62 transport [26, 27]. Litterature reviews report developments of quantitative  
 63 structure property relationships (QSPR) for polymer properties [28, 29, 30].  
 64 In the case of transparent polymeric materials, QSPR methods have been  
 65 used to model optical properties such as the refractive index,  $n$  [28, 30, 31, 32].  
 66 Holder *et al.* have shown that the use of dimeric repeating units for descriptor  
 67 calculation leads to the most accurate models [33]. Duchowicz *et al.* used a  
 68 Simplified Molecular Input Line Entry System (SMILES) – not dependent of  
 69 3D-molecular geometries – based model to predict  $n$  for 234 structurally di-  
 70 verse polymers [34]. Jabeen *et al.* developed a four-descriptor QSPR model  
 71 with accurate predictions for a highly diverse set of 133 organic polymers  
 72 [35]. Numerous works reported attempts to predict polymer properties such  
 73 as glass transition temperature,  $T_g$  using QSPR [29, 36, 37, 38, 39]. The  
 74 knowledge of  $T_g$  defines domains of rigid structure or rubber-like properties  
 75 for polymeric materials, and thus is of utmost importance for many appli-

76 cations. Mercader *et al.* have demonstrated that  $T_g$  can be well predicted  
77 with QSPR and advocated the use of trimeric moities for descriptor cal-  
78 culation [37]. QSPR were also developed to predict mechanical properties  
79 for polymeric materials [40], and Cravero *et al.* proposed QSPR models to  
80 estimate tensile strength of polymers [41]. Another possible application of  
81 QSPR modelling is to predict sorption of chemicals into polymer matrices.  
82 Zhu *et al.* proposed a QSPR based model for the prediction of diffusion  
83 coefficients of hydrophobic organic contaminants in low density polyethylene  
84 [42]. Li *et al.* proposed models for predicting polymer/brine partition co-  
85 efficients for chemicals, with polymers such as polyethylene, polypropylene  
86 and polystyrene [43]. Our group has previously proposed QSPR models to  
87 predict sorption values for neat compounds and up to quinary mixtures of  
88 hydrocarbons, alcohols, and ethers, and demonstrated their applicability to  
89 predict sorption values for some alternative fuels into a poly(ethylene) [44].

90 In the present work, we report the acquisition of new experimental sorp-  
91 tion values at room temperature for neat compounds and alternative jet fuels  
92 based fluids into three polymers. Additionally, we present QSPR based mod-  
93 els developed using machine learning methods, and its application to model  
94 new experimental data. The paper is organized as follows: we present exper-  
95 imental data methods and the strategy followed to build new QSPR based  
96 models, new experimental data and the predictive performance of models are  
97 then exposed and discussed, and the last section gives our conclusions.

## 98 2. Materials and methods

### 99 2.1. Experimental procedure

#### 100 2.1.1. Materials and Samples

101 Three polymers commonly considered for the design of fuel-delivery sys-  
102 tems were selected for this study: NBR, FKM, and FVMQ. Polymers raw  
103 materials — plane square sheets with 0.3m size and  $2 \cdot 10^{-3}$ m thickness —  
104 were supplied either by Zodiac Aerotechnics or by Stacem. Rectangular  
105 parallelepiped shapes with  $60 \times 10 \times 2 \text{ mm}^3$  were extracted from the polymer  
106 sheets using a cutting shape, and samples were subsequently used for the  
107 sorption tests. Some characteristics (grades for aerospace applications) for  
108 these materials are presented in Table 1. We also performed measurements,  
109 the Dynamic Mechanical Analysis (DMA) was used to determine the glass  
110 transition temperature for the three polymers. A sinusoidal stress was ap-  
111 plied to each sample while the strain was measured, allowing one to determine

Table 1: Characteristics for polymeric materials considered in this study.

Polymer	Type	Standards	Hardness (IRHD <sup>a</sup> )	T <sub>g</sub> (°C)	Plasticizer (% wt.)
NBR	20B8	NF L 17-120	78	-36	11.0
FVMQ	61D8	NF L 17-261	80	-55	1.2
FKM	60C8	NF L 17-164	80	-1	0.5

<sup>a</sup>IRHD: International Rubber Hardness Degree. The dial of the durometer is graduated according to the Shore D scale, from 0 (soft) to 100 (hard) IRHD, with uncertainties associated to measurements of +5/-4 IRHD.

the complex modulus and the loss factor. So-obtained T<sub>g</sub> values, reported in Table 1, correspond to the peak value of tan  $\delta$ , the damping, a measure of the energy dissipation of a material. Additionally, the Thermal Gravimetric Analysis (TGA) was used, it consists in following the mass variations of a sample with the time as the temperature changes. This measurement provides information about chemical phenomena including thermal decomposition but also physical phenomena, such as the desorption of additives. This technique has allowed the determination of the plasticizer amount initially present in each studied polymer. It led to plasticizer amounts of 0.5 % wt. for FKM, 1.2 % wt. for FVMQ, and 11 % wt. for NBR, indicating that the amount in NBR is not negligible and may lead to measurement artifacts.

Fluids under consideration in this study are pure liquids and aviation fuels. Naphthenic and aromatic hydrocarbons (decaline (labeled D), xylene (labeled X), tetraline (labeled T), iso-propylbenzene (or cumene, labeled C), n-propylbenzene (labeled P), and methylnaphtalene (labeled M)), with high purity grades were purchased from Merck, and no additional purification was performed. One Jet A-1 (labeled J) being one of the fuels most commonly used in commercial aviation was selected for sorption measurements. Additionally, we considered alternative jet fuels approved for certification such as: Synthetic Paraffinic Kerosene (SPK) and Hydroprocessed Esters and Fatty Acids (HEFA). For instance, SPK can be FT fuels — composed of normal and isoparaffins, or Alcohol to Jet Synthetic Paraffinic Kerosene (ATJ-SPK) created from isobutanol which is derived from feedstocks. HEFA — similar to HVO — includes hydrocarbon-based jet fuels (100% paraffinic) produced from animal or vegetable oils by hydroprocessing [45]. The current certification for the use of HEFA in mixture with jet fuel allows a maximum of 50%

138 vol. We considered three HEFA with different cold flow properties such as  
 139 crystallization temperatures: -50 °C, -30 °C, and -20 °C labeled H(50), H(30),  
 140 and H(20), respectively. We considered three additional fuels (labeled A1,  
 141 B1, and C1) to assess their compatibility with the polymers through sorption  
 142 measurements, and later used to assess the predictive capability of models.  
 143 A1 is a Jet A-1 fuel, noting that its composition slightly differs from that of J.  
 144 B1 is an ATJ-SPK mainly composed of i-paraffins. C1 is a jet fuel surrogate  
 145 with high aromatics content (*ca.* 20 vol%). Note that Hall *et al.* recently  
 146 considered these conventional and synthetic fuels [46], and representations  
 147 for these fluids are proposed hereafter.

148 In order to deeply explore effects of the fluid composition on polymer  
 149 mass variations when the polymer is immersed in a fluid, we defined differ-  
 150 ent mixtures varying compositions for instance, in terms of naphthenes and  
 151 aromatics content, paraffins chain length... Mixtures containing J and 25,  
 152 50, and 75 % vol. of H(50) were formulated. Nine mixtures containing H(50)  
 153 and amounts 1, 5, and 10 % vol. of X, T, and D were also elaborated. Three  
 154 blends of 90 % vol. of H(30) and 10 % vol. of C, P, and M were designed. J  
 155 was mixed with X in 75, and 25 % vol. proportions, and a ternary mixtures  
 156 containing J, X, and H(30) in equal volumetric proportions was formulated.

### 157 2.1.2. Sorption measurements

158 The term sorption is commonly used to describe the dissolution of a pen-  
 159 etrant into a polymer matrix. Measurements of liquid sorption into polymers  
 160 were performed using a gravimetric method, as detailed in our previous works  
 161 [44]. Experiments consists in recording the mass variation (weight gain or  
 162 loss) of a polymer sample with time when immersed into a large excess of  
 163 the studied liquid. Noting that from sorption values, at equilibrium or sat-  
 164 uration, it is possible to derive the solubility coefficient, and measurements  
 165 must be accurately performed as the absorbed quantities are often very small.  
 166 Rectangular parallelepiped polymer samples were first weighted ( $m_{t=0}$ ) us-  
 167 ing an analytical balance METTLER TOLEDO (capacity up to 30 g, with  
 168 a precision of 0.026 g), and then immersed in a large excess of studied liquid  
 169 in a closed 100 ml glass vessel. Glass vessels were placed at ambient temper-  
 170 ature ( $20 \pm 1$  °C) in an air-conditioned laboratory, for all the duration of the  
 171 sorption experiments. Polymer samples were regularly removed from glass  
 172 vessels, wiped carefully, and weighted ( $m_t$ ) in order to follow mass variations  
 173 of each polymer materials in considered liquids. The mass variation ( $\Delta M$ )  
 174 is expressed in percent as the ratio between the amount of sorbed fluid and

175 the initial polymer weight, as follows:

$$\Delta M = 100 \times \frac{m_t - m_{t=0}}{m_{t=0}}, \quad (1)$$

176 It has been checked that the repeatability of the sorption values is excel-  
177 lent, with less than 2% of variation coefficients. Measurements are performed  
178 until the curve  $\Delta M$  as a function of time reaches its equilibrium value, ex-  
179 hibiting a plateau. According to the considered polymer-fluid couple up to 40  
180 days were needed to reach the plateau value. We emphasize that the sample  
181 swelling has been investigated in terms of weight variations and not volume  
182 swellings as this former is assumed to be more accurate. We previously noted  
183 the presence of plasticizers in NBR which can cause a weight loss of the sam-  
184 ples during sorption tests, and can produce misleading results. Therefore, all  
185 NBR samples were pretreated to remove plasticizers, as follows: they have  
186 been washed with toluene during 3 weeks (at 50 °C to speed up the diffusion  
187 mechanism) and then dried.

## 188 2.2. Modelling Method

189 These last years, we have devoted large efforts in the development of  
190 QSPR based models for the prediction of various property values [47]. These  
191 approaches aim at identifying non-obvious correlations between property val-  
192 ues of the matter and some features rendering information about the matter.  
193 Reviews have been published dealing with developments and applications of  
194 QSPR based models, and best practices in developing such models [29, 48].

### 195 2.2.1. Data Sets

196 The accuracy of predictive QSPR is related to the quality of data, and  
197 thus a keystone of such works is the database used to develop models. The  
198 used database contains reference sorption values,  $\Delta M$  measured following the  
199 experimental procedure described above. The database contains 521 sorption  
200 values measured at room temperature, for neat compounds and mixtures.  
201 Table 2 presents an extract of our database, *i.e.* the maximum amounts of  
202 each fluid sorbed into NBR, FVMQ, and FKM. Indeed, the database contains  
203 the complete isotherms – evolution with time of the amount of sorbed fluid  
204 through NBR –, with in between 20 and 25 data points for each isotherm.

205 During last decades of QSPR model developments, the use of external  
206 validation has been shown as necessary to ensure its ability to extrapolate  
207 to new fluids, *i.e.* not considered within the database used to train the

Table 2: Maximum amounts of sorbed fluid ( $\Delta M$ , in %) into NBR, FVMQ, and FKM. Fluids are labeled as follows: X, T, D, C, P, and M stand for xylene, tetraline, decaline, iso-propylbenzene, n-propylbenzene, and methylnaphthalene, respectively ; fluids mixtures are labeled as follows, for instance, H(50)90-T10 contains 90 % vol. of H(50) in mixture with 10 % vol. of tetraline.

Label	Fluid	$\Delta M$ (%)		
		NBR	FVMQ	FKM
F01	X	120.0	9.6	6.0
F02	T	97.4	4.8	0.5
F03	D	18.7	3.6	0.0
F04	J	16.8	4.3	0.2
F05	H(20)	3.5	1.5	0.1
F06	H(50)	4.1	1.8	0.0
F07	J75-H(50)25	12.3	3.6	0.1
F08	J50-H(50)50	9.1	3.1	0.1
F09	J25-H(50)75	6.8	2.5	0.1
F10	H(50)99-X01	4.5	1.9	0.1
F11	H(50)95-X05	6.2	2.5	0.1
F12	H(50)90-X10	8.4	3.0	0.2
F13	H(50)99-T01	4.5	1.9	0.0
F14	H(50)95-T05	6.7	2.3	0.1
F15	H(50)90-T10	9.4	2.6	0.1
F16	H(50)99-D01	4.1	1.9	0.0
F17	H(50)95-D05	4.6	2.0	0.0
F18	H(50)90-D10	5.1	2.1	0.0
F19	H(30)90-C10	7.6	2.6	0.1
F20	H(30)90-P10	7.9	2.6	0.1
F21	H(30)90-M10	14.8	3.0	0.2
F22	J75-X25	30.5	6.2	0.8
F23	J25-X75	81.6	8.8	3.7
F24	J33-X33-H(30)33	27.2	5.9	0.8

208 model [49]. Its popular version is the  $n$ -fold cross-validation ( $n$ -CV) in which  
 209 the data set is randomly divided in approximately equal  $n$  portions. An  
 210 aggregate of  $(n-1)$  portions forms the Training set – used to train models,  
 211 and the remaining portion constitutes the Test set – used to evaluate model’s  
 212 performance. We emphasize that no data point belonging to external sets  
 213 is used to derived models. This procedure is repeated  $n$  times choosing at  
 214 each new fold another portion of data as a Test set. The subject of external  
 215 validation for QSPR analysis of mixtures has been addressed by Muratov *et*  
 216 *al.* [50], and the authors-defined ”mixture out” strategy was applied in this  
 217 study.

### 218 2.2.2. *Fluids characterisation and representation*

219 A fuel contains thousands of diverse chemicals and its exact composition is  
 220 never known. The characterization of such complex fluids and identification  
 221 of representative compounds or surrogates are of utmost importance when  
 222 developing predictive models for application in the industry [51, 52]. The use  
 223 of modern analytical instruments such as chromatography, helps in obtaining  
 224 information about the composition and structure of fluids components. The  
 225 two-dimensional gas chromatography (labeled GC-2D or GCxGC) has been  
 226 proved as an interesting analysis technique for detailed characterisation of  
 227 petroleum products [53]. Fuel candidates considered in this study were ana-  
 228 lyzed by means of GCxGC, and their compositions expressed as distributions  
 229 of mass fractions as a function of the number of carbon atoms for hydrocarbon  
 230 families such as n-paraffins, i-paraffins, naphthenes, aromatics... A molecu-  
 231 lar structure is attributed for each hydrocarbon family/number of carbon  
 232 atom bin, and each fuel is thus represented by a maximum of 120 molecular  
 233 structures. Figure 1 presents compositions of fluids A1, B1, C1, J, H(20),  
 234 H(30), and H(50), simplified to four chemical families: n-paraffins, i-paraffins,  
 235 naphthenes, and aromatics. It shows that ATJ-SPK (B1) and HEFA fuels  
 236 are clearly mainly paraffinics, with B1 purely n-paraffinics. A1 and J have  
 237 similar compositions with for J, slightly (*ca.* 3 %) lower and higher i-paraffins  
 238 and aromatics contents, respectively. The surrogate C1 is poor in paraffins  
 239 and rich in naphthenes as compared to other fluids.

### 240 2.2.3. *Molecular and mixture descriptors*

241 From conclusions drawn in previous studies [2, 44], we chose to solely  
 242 consider functional group count descriptors (FGCD). Such a simple repre-  
 243 sentation of compounds has been shown to provide relevant descriptors us-

Table 3: Ranges of number of carbon atoms to represent jet fuel candidates.

Formulae	Family	Number of C atoms
$C_nH_{2n+2}$	n-paraffins	5 to 20
$C_nH_{2n+2}$	i-paraffins	5 to 30
$C_nH_{2n}$	mono-naphthenes	6 to 18
$C_nH_{2n-2}$	di-naphthenes	9 to 29
$C_nH_{2n-4}$	tri-naphthenes	13 to 16
$C_nH_{2n-6}$	mono-aromatics	7 to 17
$C_nH_{2n-8}$	naphthenes mono-aromatics	9 to 16
$C_nH_{2n-10}$	naphthenes mono-aromatics	10 to 15
$C_nH_{2n-12}$	di-aromatics	10 to 16
$C_nH_{2n-14}$	naphthenes di-aromatics	12 to 16
$C_nH_{2n-16}$	naphthenes di-aromatics	13 to 15

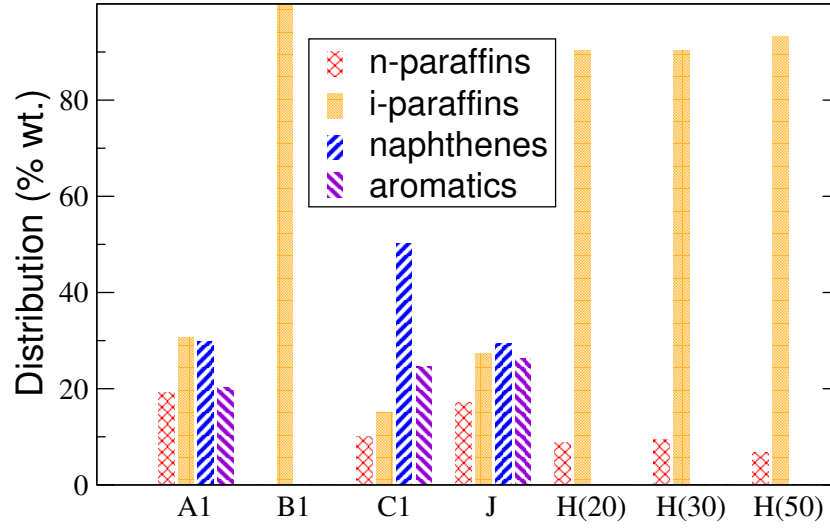


Figure 1: Simplified chemical compositions described in terms of n-paraffins, i-paraffins, naphthenes, and aromatics, for fluids A1, B1, C1, J, H(20), H(30), and H(50).

Table 4: List of the Functional Group Count Descriptors (FGCD) used to describe fluids in the database and associated SMARTS codes or definitions.

Label	SMARTS/Definition	Label	SMARTS/Definition
X1	[H]	X18	[C][CR](![C])(![C])[C]
X2	[C,c]	X19	[C][CR](![C])([C])[C]
X3	[CX4H3]	X20	[C]=[C]([C])![C]
X4	[CX4H2]	X21	[CX3H1]=[CX3H1]
X5	[CX4H1]	X22	[c][CX4H3]
X6	[CX4H0]	X23	[c][CX4H2]
X7	[CX3H1]	X24	[c][CX4H1]
X8	[CX4H2R]	X25	[R]
X9	[CX4H1R]	X26	aromatic_rings
X10	[cX3H1](:*):*	X27	non-aromatic_rings
X11	[cX3H0](:*)(:*)*	X28	aliphatic_rings
X12	[cX3H0](:*)(:*):*	X29	number_of_rings
X13	[cX3H0]-[CX3]	X30	MM
X14	[cX3H0](:*)(:*)(-[CX4H2R])	X31	[C;R]
X15	[CX4H2]-[CX4H1]-[CX4H2]	X32	[c;R]
X16	[C][C]([CX1])([CX1])![CX1]	X33	C1CCCCC1
X17	![C][C]([C])([C])[C]		

able in QSPR procedure [3, 44]. This family of molecular descriptors gathers some counts of groups identified as relevant under chemical aspects. Table 4 gives the list of FGCD under consideration in this study and labelled from X1 to X33. For instance, the FGCD labelled X25 denotes the number of carbon atoms involved in a ring. As Villanueva *et al.* did [44], we have also computed the molar mass (MM) of neat compounds, this information being used as an additional descriptor (labelled X30). Simplified molecular input line entry specification (SMILES) notations were assigned to each neat compound considered in this study. FGCD were counted using the RDKit’s SMILES arbitrary target specification (SMARTS) matching functionalities [54, 55], and SMARTS codes corresponding to FGCD are given in Table 4.

The calculation of descriptors for mixtures has been addressed similarly as in previous works [44, 56]. We assumed mixture descriptors  $X_{mix}$  as linear combinations of pure component descriptors weighted with the associated molar fractions  $x_i$ . This approach has already been shown effective in pre-

dicting sorption values for some alternative fuels in a poly(ethylene) [44].  
 For instance, in the case of descriptor X1, the corresponding descriptor for a  
 mixture X1<sub>mix</sub>, is defined as follows:

$$X1_{mix} = \sum_{i=1}^N x_i \times X1_i, \quad (2)$$

where  $i$  runs over the  $N$  constituents in the mixture.

#### 2.2.4. Chemical space representation

We preprocessed the data by applying a principal component analysis (PCA) on fluid descriptor values. Figure 2 represents the projections of F01 to F24 in the space formed by the three main principal components resulting from the PCA, providing one approximated representation of the chemical space for our database. Some of fluid candidates are at edges of the domain, isolated from all other samples, this is typically the case for fluids F01, F03, F04, and F05. These latter datapoints appear as outliers for the following reasons: (i) F01, xylene, is a pure compound with the highest property value ; (ii) F03, decaline, is a pure compound and has the highest value on PC2 axis ; (iii) F04, Jet-A1, has the highest value on PC3 axis ; (iv) F05, HEFA-20, has the lowest property value. The presence of outliers in external sets during the CV procedure may induce applicability domain violations. Fluids F01, F03, F04, and F05 were fixed, meaning they are placed in a fold always used to form Training sets. We used a 5-CV procedure applied on the remaining 20 fluids candidates – four fluids per fold. The Training and Test sets thus represent 83% and 17% of the database, respectively. In Figure 2, each symbol is filled according to the fold the fluid belongs to.

#### 2.2.5. Machine learning algorithm

In the frame of past studies [47], we have observed that QSPR models derived from Support Vector Machine (SVM) algorithms frequently outperform others evaluated learning algorithms such as neural networks, partial least squares, genetic algorithm... Table 2 shows that the number of data points – fluids candidates – is quite limited and the application of SVM does not seem appropriate in this case. We focused on developing multilinear equations which moreover have the advantage to be explicit models and easily implemented in a spreadsheet. Such multilinear models can be, for instance, generated by means of Evolutionary Algorithms (EA) techniques inspired

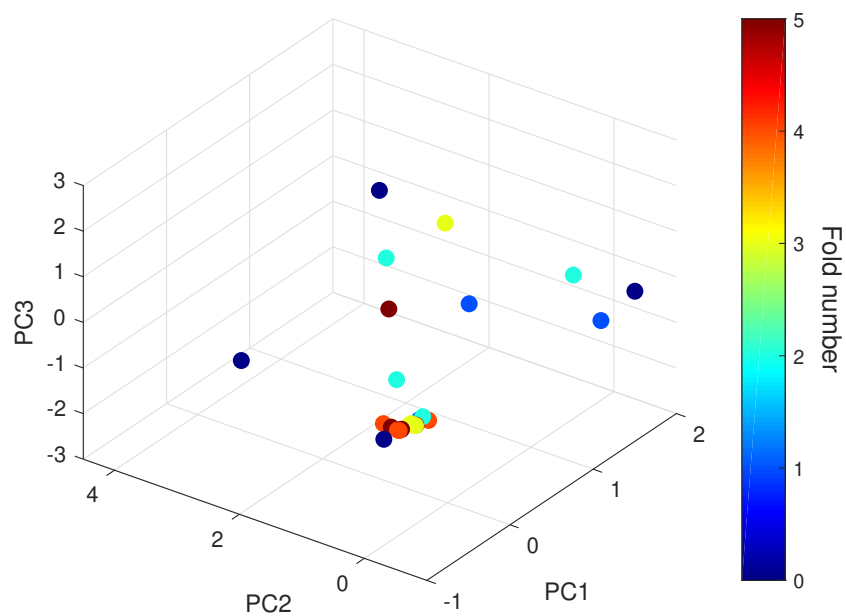


Figure 2: Projections of jet fuel based fluids on the space formed by PC1, PC2 and PC3, the three first principal components resulting from the PCA. Symbols are filled according to a gradient of colors, as legended in the colorbar each of the six folds is represented by one color.

291 from the Darwinian evolution theory of biological species. The application  
 292 of EA to regression problems consists in an iterative evolution of a population  
 293 of equations initially randomly set. Equations can be summarized under the  
 294 general following form:

$$Property = \lambda_0 + \sum_{i=1}^N \lambda_i G_i, \quad (3)$$

295 where  $\lambda_0$  is the inercept,  $\lambda_i$  denotes a weight associated to the gene  $i$  ( $G_i$ ),  
 296 and  $N$  is the total number of genes in the model. Each gene consists in a  
 297 combination of descriptors (see Table 4) and mathematical functions (see Ta-  
 298 ble 5), and can be though as a tree with nodes and branches (Figure 3). Such  
 299 construction allows to catch non-linearity in property variations. Multi-Gene  
 300 Genetic Programming (MGGP) was applied to generate models, using the  
 301 genetic programming toolbox for the identification of physical systems (GP-  
 302 TIPS) coded in the MATLAB environment [57, 58, 59]. The evolution of the  
 303 initial population – initial equations – is ensured by survival of fitter individ-  
 304 uals, and reproduction of individuals consists in applying crossover as well as  
 305 mutation operations to produce child equations. Genetic operators act upon  
 306 sub-tree elements, thus making the structure of trees evolve during the itera-  
 307 tive procedure. The procedure ends when one of the pre-defined criteria such  
 308 as maximum number of generations, best fitness values... is reached. Some  
 309 of GPTIPS parameters such as the maximum numbers of genes and nodes  
 310 per tree, must be lowered to prevent any overfitting problems. Similarly, the  
 311 maximum numbers of generations and runs have to be optimized to ensure  
 312 convergence of calculations for reasonable computational ressources [60, 61].  
 313 Parameters of performed GPTIPS calculations were optimized according to  
 314 the procedure defined by Creton *et al.* [60]. Table 5 reports details about  
 315 values and/or ranges of investigated GPTIPS settings in this work.

316 Models are evaluated according to their capability in predicting fluids  
 317 properties. Predicted values are compared to reference experimental data,  
 318 and performances of models are evaluated by means of metrics such as MAE  
 319 (Mean Absolute Error, equation (4)), RMSE (Root Mean Squared Error,  
 320 equation (5)) or  $R^2$  (Coefficient of determination, equation (6)), defined as  
 321 follows:

$$MAE = \frac{1}{N} \sum_{i=1}^N |\hat{y}_i - y_i|, \quad (4)$$

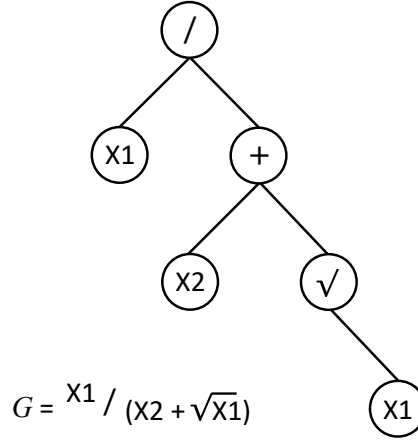


Figure 3: Example of a gene  $G$ , and its tree-like architecture as considered in MGGP.

Table 5: Investigated parameter settings for the MGGP based method.	
Parameter	Corresponding values
Function set	+, -, ×, ÷, √, exp, ln
Population size	250
Number of runs	1, 5, 10, 15, 20, 25, 30, 40
Tournament size	25
Maximum tree depth	4
Number of generations	100, 500, 1000, 2000
Maximum number of genes	1 to 5
Maximum number of nodes per tree	1 to 8
Mutation events	0.1
Crossover events	0.85
Reproduction events	0.05

$$\text{RMSE} = \sqrt{\frac{1}{N} \sum_{i=1}^N (\hat{y}_i - y_i)^2}, \quad (5)$$

$$R^2 = \frac{\sum_{i=1}^N (\hat{y}_i - \bar{y})^2}{\sum_{i=1}^N (y_i - \bar{y})^2}, \quad (6)$$

where in equations (4) to (6),  $\hat{y}_i$  stands for the predicted value,  $y_i$  represents the experimental value,  $\bar{y}$  denotes the mean property value calculated on experimental data set candidates, and  $N$  is the number of data.

### 3. Results and discussion

#### 3.1. Experimental results

We performed sorption experiments to evaluate polymers (*i.e.*, NBR, FVMQ, and FKM) compatibility with a series of hydrocarbons mixtures and more specially, to mixtures containing different amounts and types of aromatics. Details about tested fluids mixtures are given in the Table 2. The weight variation of the polymer is very dependent on the considered system, the chemical compositions of both the polymer and the fluid. The measured maximum uptakes of hydrocarbons in each polymer (or maximum  $\Delta M$ ) are presented in Table 2. From tested polymer/fluid couples,  $\Delta M$  values range from *ca.* 0% (FKM immersed in HEFA) to 120% (NBR immersed in xylene). Clearly, none of tested hydrocarbons is significantly absorbed into FKM, and from measured values, FKM can be assumed as a barrier polymer in case of hydrocarboned fluids.  $\Delta M$  values obtained for the FVMQ polymer are negligible as compared to those of NBR. Within the fluids matrix (Table 2), we considered mixtures having from about 0% vol. aromatics (*e.g.*, HEFA) to 100% vol. aromatics (*e.g.*, xylene). In Figure 4, we plot the  $\Delta M$  plateau value for NBR as a function of mono-aromatics content in the fluid tested. Considering all these systems, deplasticized NBR presents a higher level of sorption and is very sensitive to the aromatics content of the fluids. Figure 4 shows that mixtures rich in paraffins such as HEFA fuels (left part of the diagram) lead to low  $\Delta M$  values as compared to mono-aromatics rich mixtures (right part of the diagram). From these elements a quadratic (of the % vol. of mono-aromatics) trend could describe the observed behavior. Noting that fluids containing polyaromatic compounds, *e.g.* the fluid F21 containing 10% vol. methylnaphtalene, deviate from this trend with upper  $\Delta M$  values.

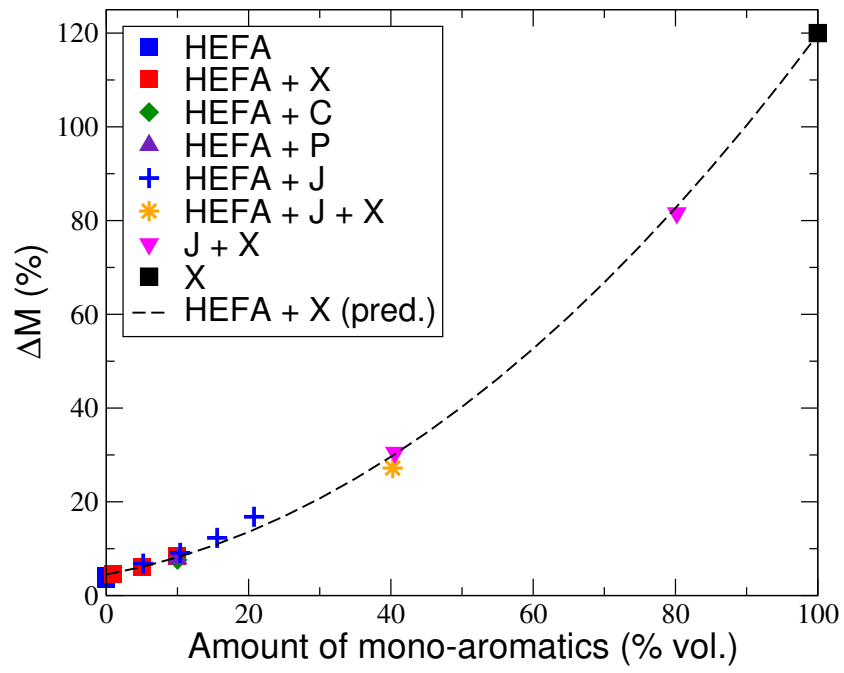


Figure 4: Evolution of the  $\Delta M$  plateau value for NBR, with the mono-aromatics volumetric percent of the fluid. Fluids are labeled as in Table 2: X, C, P, and J stand for xylene, iso-propylbenzene, n-propylbenzene, and Jet-A1, respectively. The dashed line stands for values predicted using equation 7.

Table 6: Maximum amounts of sorbed ( $\Delta M$ ) A1, B1, and C1 into NBR, FVMQ, and FKM.

Fluid	$\Delta M$ (%)		
	NBR	FVMQ	FKM
A1	14.2	4.7	0.3
B1	2.7	4.4	0.1
C1	30	3.9	0.4

Fluids A1, B1 and C1 — conventional and synthetic jet fuels — were considered to experimentally assess their compatibility with the three polymers of interest, and Table 6 presents measured  $\Delta M$  values. In agreement with conclusions drawn previously, amounts of fluids adsorbed into FKM or FVMQ are roughly much lower than that measured for NBR. On the basis of compositions proposed in Figure 1 for A1, B1, and C1,  $\Delta M$  plateau values appear to follow the previously observed relationships with paraffins and aromatics contents.

### 3.2. Machine learning models

Obtained experimental values were used to feed machine learning techniques in order to derive predictive models. Based on the conclusions drawn in the previous section, small quantities of hydrocarbons were adsorbed into FKM and FVMQ and therefore, we only focus on modelling of the sorption of hydrocarbons into NBR. We hereafter report the development of two types of predictive models: models which predict the maximum mass gain (maximum  $\Delta M$ ) and models which predict the sorption kinetics *i.e.* the time evolution of  $\Delta M$ , in NBR.

#### 3.2.1. Modelling plateau values

As a first attempt, we considered a subpart of our database extracting for each fluid the sorption plateau value — the maximum mass percentage gain —, and data are presented in Table 2. Parameters of the MGGP such as numbers of runs, generations, genes, and nodes that will further be used to develop models were optimized using a 5-CV and according to the procedure proposed by Creton *et al.* [60]. This procedure can be summarized as follows: The numbers of genes and nodes are first set to their respective maximum allowed value to consider models having the highest complexity. Numbers of

Table 7: Performance characteristics (statistical indices) of MGGP based models applied to plateau values. Fold- $i$  stands for performances calculated on the fold  $i$  when it is external to the learning procedure.

Indices	Fold-01	Fold-02	Fold-03	Fold-04	Fold-05
MAE	9.21	1.90	0.63	1.60	0.42
RMSE	17.23	2.87	0.75	2.80	0.54
R <sup>2</sup>	0.786	0.992	0.995	0.614	0.929

generations and runs are optimized within the response surface with boundaries as defined in Table 5. Then, numbers of generations and runs are set to optimized values, and numbers of genes and nodes are optimized within the response surface defined according to boundaries indicated in Table 5. The optimization procedure applied to our regression problem led to numbers of runs, generations, genes, and nodes of 20, 500, 4, and 3, respectively.

Five MGGP based models were developed using the GPTIPS code and following a 5-fold cross-validation procedure. All models exhibit excellent performances over the Training sets. Performances of models evaluated on external fluids are presented in Table 7. Values returned by indices for Fold-01 and Fold-04 indicate overfitting trends for these two models that can originate from fold constitution. For instance, Fold-01 contains the fluid F02 having the second highest property value in the database, and the model fails in predicting this value. Among the three remaining models, best performances on external sets are obtained for Fold-05, Fold-03, and then Fold-02. However, the chemical diversity is not similar for these three folds. The model that best generalizes the database has been developed using Fold-02 as Test set. Details about this latter model such as the four weighted genes and the intercept value are presented in Equation (7).

$$\begin{aligned}
\lambda_0 &= \text{Intercept} = -30.12 \\
\lambda_1 G_1 &= -36.70 * \exp(-\exp(-X4)) \\
\lambda_2 G_2 &= 70.87 * \exp(X26) \\
\lambda_3 G_3 &= -12.38 * \sqrt[4]{X21} \\
\lambda_4 G_4 &= 7.26 * \exp(X33 - X10)
\end{aligned} \tag{7}$$

where  $X_i$  stands for descriptors as defined in the Table 4. In Equation (7),

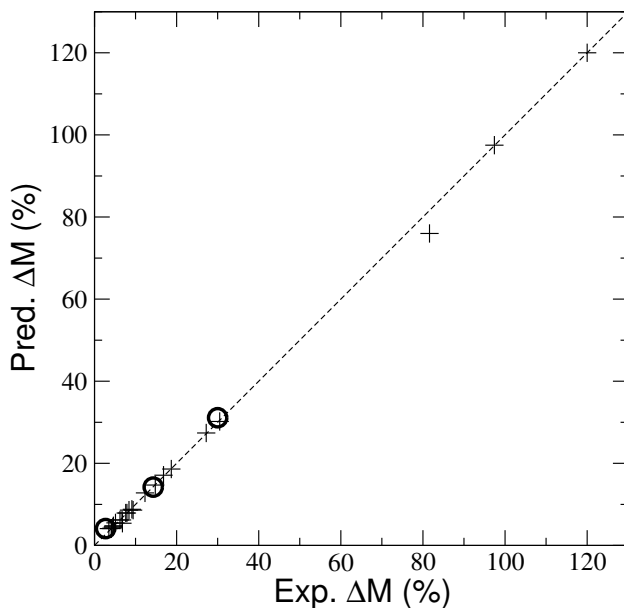


Figure 5: Scatterplots of experimental sorption values *vs.* predicted sorption values using Equation (7). Symbols + stand for fluids in Table 2, and  $\bigcirc$  represent fuels A1, B1, and C1.

397 each gene non-linearly contributes to the predicted sorption value, and Equa-  
 398 tion (7) highlights some interesting contributions of chemical function to the  
 399 amount of fluid sorbed into NBR. For instance, Equation (7) indicates that  
 400 increasing the number of  $-\text{CH}_2-$  groups (X4) in fluid decreases the sorption  
 401 value. On the contrary, increasing the number of aromatic rings (X26) in  
 402 fluid increases its amount sorbed into NBR. These elements are in line with  
 403 the analysis of Figure 4.  $G_4$  is a combination between numbers of saturated  
 404 6-rings (X33) and hydrogenated aromatic carbon atom bonded to two atoms  
 405 by aromatic bonds (X10). Figure 5 presents scatterplots of experimental  
 406 sorption values *vs.* predicted sorption values using equation (7). All data  
 407 points are roughly located on the bisector (dashed line) indicating that pre-  
 408 dicted plateau values are in excellent agreement with reference experimental  
 409 data. Moreover, values predicted for fuels A1, B1, and C1 (14.2, 4.1, and  
 410 31.1, respectively) are in excellent agreement with corresponding experimen-  
 411 tal values as reported in Table 6.

Table 8: Optimized parameter settings used to train MGGP based models on our database.

Parameter	Optimized values
Number of runs	20
Number of generations	1000
Maximum number of genes	4
Maximum number of nodes	6

### 3.2.2. Modelling the sorption kinetic

We then considered the whole content of our database with for each fluid, the time evolution of the maximum mass percentage gain. Parameters of the MGGP as implemented in the GPTIPS code were optimized according to the procedure proposed by Creton *et al.* [60]. Additionally, we applied a 5-CV procedure together with folds’ chemistry — the same fluids in each fold — associated to the above described development of models to predict plateau values. Table 8 presents obtained optimized parameter values subsequently used in GPTIPS to develop QSPR models. The number of nodes is twice higher as compared to parameters values optimized to derive Equation (7), and most probably due to this increase in complexity, the number of generations is here 1000.

Five MGGP based models were developed removing for each, one of the five folds defined for the 5-CV procedure. Performances of models evaluated on the Training and Test (external fluids) sets are presented in Table 9. All models exhibit excellent performances over the Training sets with RMSE lower than 2.6 (in  $\Delta M$  unit) and  $R^2$  greater than 0.99. Indices calculated for Test sets of models indicate various trends regarding their predictive capabilities. However, as discussed previously, the chemical diversity is not similar within the five folds, and external validation performed for these five scenarios are difficult to compare with each other. Values taken by indices over the database are presented in Table 9. Considering these latter values, the model developed using Fold-01 as Test set leads to a greater RMSE value as compared to others. Although none of models outperforms others, the model that best generalizes the database was obtained using Fold-05 as Test set. Details about this latter model such as the four weighted genes and the intercept value are presented in Equation (8).

Table 9: Performance characteristics (statistical indices) of MGGP based models applied to sorption curves. Fold- $i$  stands for performances calculated on the fold  $i$  when it is external to the learning procedure.

Metrics	Fold-01	Fold-02	Fold-03	Fold-04	Fold-05
Training:					
MAE	1.02	1.29	1.52	1.49	1.38
RMSE	1.82	2.45	2.56	2.52	2.53
R <sup>2</sup>	0.995	0.992	0.993	0.993	0.993
Test:					
MAE	2.96	1.42	1.27	1.54	0.69
RMSE	5.54	2.63	1.64	2.24	0.96
R <sup>2</sup>	0.975	0.992	0.978	0.776	0.859
Database:					
MAE	1.34	1.31	1.48	1.50	1.26
RMSE	2.80	2.48	2.42	2.48	2.34
R <sup>2</sup>	0.990	0.992	0.992	0.992	0.993

$$\begin{aligned}
\lambda_0 = \text{Intercept} &= -38.40 \\
\lambda_1 G_1 &= 12.23 * \exp(\exp(X26)) \\
\lambda_2 G_2 &= 0.86 * (X9^4 + X22^3) \\
\lambda_3 G_3 &= 4.51 * \sqrt{\exp(X10) * \ln(t)} \\
\lambda_4 G_4 &= -2.35 * \exp(X10)
\end{aligned} \tag{8}$$

439 where  $t$  is the time (expressed in hours) and  $X_i$  stands for descriptors as  
 440 defined in Table 4. In Equation (8),  $G_1$  reveals that increasing the number  
 441 of aromatic rings (X26) in fluid increases its amount sorbed into NBR.  $G_2$   
 442 can be considered as a sum of contributions of branchings on saturated (X9)  
 443 and aromatic (X22) rings. The descriptor X10 – number of hydrogenated  
 444 aromatic carbon atom bonded to two atoms by aromatic bonds – is involved  
 445 both in genes  $G_3$  and  $G_4$  where in this former, X10 acts as a weight for the  
 446 time evolution. Figure 6 presents scatterplots of experimental sorption values  
 447 *vs.* predicted sorption values using Equation (8). All data points are not too  
 448 scattered on both sides of the bisector indicating that predicted values are in  
 449 good agreement with reference experimental data. However, Figure 6 shows

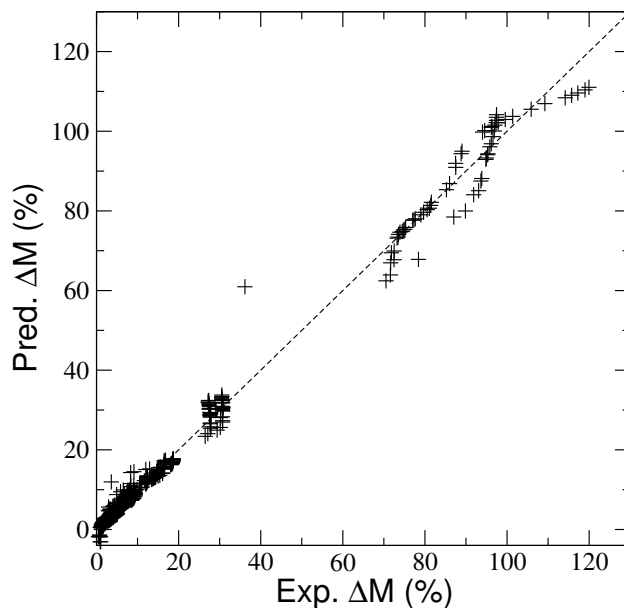


Figure 6: Scatterplots of experimental sorption values *vs.* predicted sorption values using Equation (8).

450 that one point is poorly predicted, the sorption value measured after 5 hours  
 451 immersion in tetraline is 36.1 (%) while the model returns 61 (%). Noting  
 452 that for tetraline, only this data point is poorly predicted.

453 We performed consensus modelling to investigate whether combining mod-  
 454 els' predictions can lead to more accurate predicted values. It reveals that  
 455 combining predictions of models obtained using Fold-04 and Fold-05 as Test  
 456 sets improve performances as compared to individual models. We used this  
 457 combinaison to predict the time evolutions of sorption values for real fuels  
 458 A1, B1, and C1. Figure 7 presents comparisons between predicted values and  
 459 experimental data measured in this study. The models successfully reproduce  
 460 the sorption kinetics for the fluids A1 and C1, with however significant devi-  
 461 ations from experimental values for the first hours. The models well predict  
 462 B1 as a low ingress fluid in NBR but a shift of few percents is observed with  
 463 reference experimental values.

#### 464 4. Conclusion

465 We proposed here an investigation of fuels' sorption into polymers by  
 466 means of experimental and machine learning techniques. Three polymers

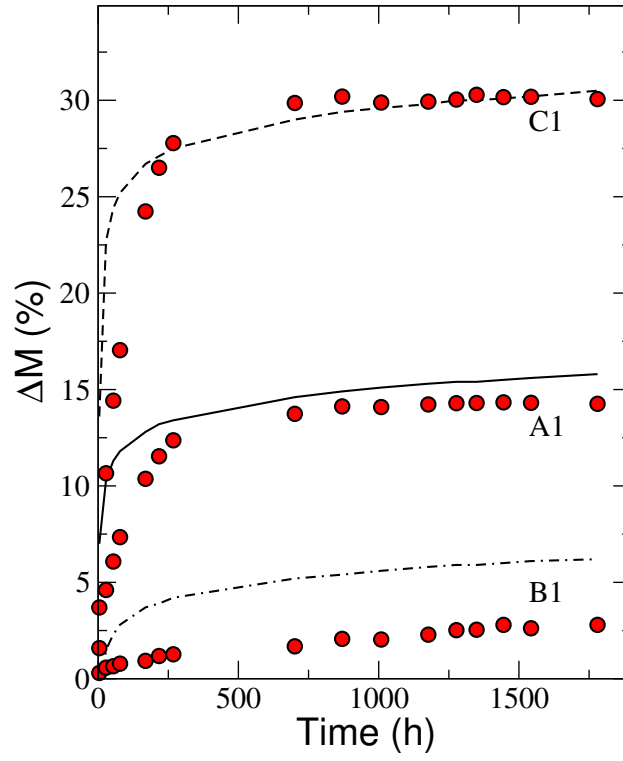


Figure 7: Time evolutions of sorption values for fuels A1, B1, and C1 predicted using the consensus model. Red circles stand for experimental values obtained in this work.

commonly considered for the design of fuel-delivery systems were selected for this study: NBR, FKM, and FVMQ. Polymers samples were immersed into liquids, and fluids under consideration were pure liquids and aviation fuels — conventional and synthetic jet fuels. Sorption measurements were performed for polymer/fluid couples, and experimental values were analysed with chemoinformatics tools, and a machine learning method (*i.e.* MGGP) and molecular descriptors (*i.e.* FGCD) were used to derive predictive models.

Performed sorption experiments to evaluate NBR, FVMQ, and FKM compatibility with a series of hydrocarbons mixtures, have shown that FKM can be assumed as a barrier polymer in case of such fluids, and that  $\Delta M$  values obtained for the FVMQ are small as compared to those for NBR. If *n*- and iso-paraffins are fewly ingress into the NBR matrix, we demonstrated that the swelling of NBR is strongly related to the amount of aromatics in the studied liquids.

Machine learning techniques were used to derive two types of predictive models. The first type of models aimed in predicting plateau  $\Delta M$  values, the maximum mass percentage gains. Models successfully reproduced experimental data, and indicate that increasing the number of  $-\text{CH}_2-$  groups and aromatic rings in the fluid leads to decreasing and increasing the amount of liquid sorbed into NBR, respectively. Application of the models to external multi-component mixtures (not considered during the training procedure) have demonstrated their predictive capabilities. The second type of models aimed in predicting the sorption kinetics, *i.e.* the time evolution of  $\Delta M$ . Models reasonably reproduced experimental data, and in these models too, increasing the number of aromatic rings in fluid contributes in increasing predicted values of  $\Delta M$ , in NBR. Application of these models to external fluids have demonstrated their capabilities in predicting both the kinetics and the maximum  $\Delta M$  values.

The determination of gases and liquids sorption into polymers is fundamental in many applications: fuels, lubricants, packaging, gas and liquids transport and storage, among others. Our work shows that when using a good quality database and relevant descriptions of fluids, machine learning approaches are capable to catch sorption phenomenon, and the so-obtained predictive models are powerful tools to accurately estimate the sorption of chemicals into a polymer. Moreover, such a modelling approach contributes to drastically reduce the time necessary to quantify polymeric materials compatibility with a fluid candidate only knowing some of its structural characteristics. This work is to be extended to other families of polymers and

505 fluids, as well as to explore new conditions of temperature and pressure. The  
 506 use of such models is interesting for assessing the impact of advanced fuels  
 507 formulations, for evaluating the impact of certain chemical families, or even  
 508 for determining the maximum amounts of biomass-based fluids into fuels.  
 509 In addition, these models could be used to replace the current qualitative  
 510 information — green, orange, and red symbols — in polymer compatibility  
 511 charts provided by resellers on their websites. The inversion of models based  
 512 on machine learning represents another interesting prospect for the design of  
 513 new polymers with desired properties [62, 63, 64].

## 514 **Acknowledgement**

515 Authors greatly acknowledge Maira Alves-Fortunato, Axel Baroni, Arij  
 516 Ben Amara, Xavier Martin, Mickael Matrat, Laurie Starck for the fruitful  
 517 discussions. The research presented in this paper has been performed in the  
 518 framework of: (i) the European project JETSCREEN (JET fuel SCREENing  
 519 and optimization), and has received funding from the European Union Hori-  
 520 zon 2020 Programme under grant agreement no. 723525 ; (ii) and the French  
 521 national research program entitled CAER (Alternative Fuels for Aeronautics)  
 522 supported by French Directorate-General for Civil Aviation (DGAC).

## 523 **References**

- 524 [1] H. K. Jeswani, A. Chilvers, A. Azapagic, Environmental sustainability  
 525 of biofuels: a review, *Proceedings of the Royal Society A: Mathematical,*  
 526 *Physical and Engineering Sciences* 476 (2020) 20200351.
- 527 [2] D. A. Saldana, B. Creton, P. Mougin, N. Jeuland, B. Rousseau,  
 528 L. Starck, Rational formulation of alternative fuels using QSPR meth-  
 529 ods: Application to jet fuels, *Oil Gas Sci. Technol. - Rev. IFP Energies*  
 530 *nouvelles* 68 (2013) 651–662.
- 531 [3] D. A. Saldana, L. Starck, P. Mougin, B. Rousseau, L. Pidol, N. Jeu-  
 532 land, B. Creton, Flash point and cetane number predictions for fuel  
 533 compounds using quantitative structure property relationship (QSPR)  
 534 methods, *Energy & Fuels* 25 (2011) 3900–3908.
- 535 [4] H. Schulz, Short history and present trends of fischer-tropsch synthesis,  
 536 *Applied Catalysis A: General* 186 (1999) 3–12.

- 537 [5] K. Murata, Y. Liu, M. Inaba, I. Takahara, Production of synthetic  
538 diesel by hydrotreatment of jatropha oils using Pt-Re/H-ZSM-5 catalyst,  
539 Energy & Fuels 24 (2010) 2404–2409.
- 540 [6] W. Weiss, H. Dulot, A. Quignard, N. Charon, M. Courtiade, Direct coal  
541 to liquids (DCL): High quality jet fuels, in: 27th Annual International  
542 Pittsburgh Coal Conference, 2010.
- 543 [7] T. R. Carlson, G. A. Tompsett, W. C. Conner, G. W. Huber, Aromatic  
544 production from catalytic fast pyrolysis of biomass-derived feedstocks,  
545 Topics in Catalysis 52 (2009) 241–252.
- 546 [8] S. Akhlaghi, U. W. Gedde, M. S. Hedenqvist, M. T. Conde Braña,  
547 M. Bellander, Deterioration of automotive rubbers in liquid biofuels:  
548 A review, Renewable and Sustainable Energy Reviews 43 (2015) 1238–  
549 1248.
- 550 [9] X.-F. Wei, L. De Vico, P. Larroche, K. J. Kallio, S. Bruder, M. Bellander,  
551 U. W. Gedde, M. S. Hedenqvist, Ageing properties and polymer/fuel  
552 interactions of polyamide 12 exposed to (bio)diesel at high temperature,  
553 npj Materials Degradation 3 (2019) 1.
- 554 [10] P. M. Subramanian, Polymer Blends, American Chemical Society, Wash-  
555 ington, DC, 1990, pp. 252–265. doi:10.1021/bk-1990-0423.ch013.
- 556 [11] S. M. Alves, V. S. E. Mello, F. K. Dutra-Pereira, Biodiesel com-  
557 patibility with elastomers and steel, in: E. Jacob-Lopes, L. Queiroz  
558 Zepka (Eds.), Frontiers in bioenergy and biofuels, InTech, Rijeka, 2017.  
559 doi:10.5772/65551.
- 560 [12] P. Izák, L. Bartovská, K. Friess, M. Šípek, P. Uchýtil, Comparison of  
561 various models for transport of binary mixtures through dense polymer  
562 membrane, Polymer 44 (2003) 2679–2687.
- 563 [13] A. Randová, L. Bartovská, K. Friess, Š. Hovorka, P. Izák, Fundamental  
564 study of sorption of pure liquids and liquid mixtures into polymeric  
565 membrane, European Polymer Journal 61 (2014) 64–71.
- 566 [14] A. Randová, L. Bartovská, P. Izák, K. Friess, A new prediction method  
567 for organic liquids sorption into polymers, Journal of Membrane Science  
568 475 (2015) 545–551.

- [15] L. Krajakova, M. Laskova, J. Chmelar, K. Jindrova, J. Kosek, Sorption of liquid diluents in polyethylene: Comprehensive experimental data for slurry polymerization, *Industrial & Engineering Chemistry Research* 58 (2019) 7037–7043.
- [16] A. Haseeb, M. A. Fazal, M. I. Jahirul, H. H. Masjuki, Compatibility of automotive materials in biodiesel: A review, *Fuel* 90 (2011) 922–931.
- [17] A. Haseeb, T. S. Jun, M. A. Fazal, H. H. Masjuki, Degradation of physical properties of different elastomers upon exposure to palm biodiesel, *Energy* 36 (2011) 1814–1819.
- [18] M. D. Kass, T. Theiss, S. Pawel, J. Baustian, L. Wolf, W. Koch, C. Janke, Compatibility assessment of elastomer materials to test fuels representing gasoline blends containing ethanol and isobutanol, *SAE Int. J. Fuels Lubr.* 7 (2014) 445–456.
- [19] L. M. Silva, E. G. Filho, A. J. Simpson, M. R. Monteiro, T. Venâncio, Comprehensive multiphase NMR spectroscopy: A new analytical method to study the effect of biodiesel blends on the structure of commercial rubbers, *Fuel* 166 (2016) 436–445.
- [20] W. Trakarnpruk, S. Porntangjitlikit, Palm oil biodiesel synthesized with potassium loaded calcined hydrotalcite and effect of biodiesel blend on elastomer properties, *Renewable Energy* 33 (2008) 1558–1563.
- [21] M. Weltschev, F. Heming, M. Haufe, M. Heyer, The influence of the age of biodiesel and heating oil with 10 % biodiesel on the resistance of sealing materials at different temperatures, *Materialwissenschaft und Werkstofftechnik* 48 (2017) 837–845.
- [22] A. Plota, A. Masek, Lifetime prediction methods for degradable polymeric materials? a short review, *Materials* 13 (2020) 4507.
- [23] N. Nosengo, Can artificial intelligence create the next wonder material?, *Nature* 533 (2016) 22–25.
- [24] Y. Liu, Z. Hu, Z. Suo, L. Hu, L. Feng, X. Gong, Y. Liu, J. Zhang, High-throughput experiments facilitate materials innovation: A review, *Science China Technological Sciences* 62 (2019) 521–545.

- 600 [25] Y. Liu, O. C. Esan, Z. Pan, L. An, Machine learning for advanced energy  
601 materials, *Energy and AI* 3 (2021) 100049.
- 602 [26] D. J. Audus, J. J. de Pablo, Polymer informatics: Opportunities and  
603 challenges, *ACS Macro Letters* (2017) 1078–1082.
- 604 [27] L. Chen, G. Pilania, R. Batra, T. D. Huan, C. Kim, C. Kuenneth,  
605 R. Ramprasad, Polymer informatics: Current status and critical next  
606 steps, *Materials Science and Engineering: R: Reports* 144 (2021) 100595.
- 607 [28] A. R. Katritzky, S. Sild, M. Karelson, Correlation and prediction of the  
608 refractive indices of polymers by QSPR, *Journal of Chemical Informa-  
609 tion and Computer Sciences* 38 (1998) 1171–1176.
- 610 [29] A. R. Katritzky, M. Kuanar, S. Slavov, C. D. Hall, M. Karelson, I. Kahn,  
611 D. A. Dobchev, Quantitative correlation of physical and chemical prop-  
612 erties with chemical structure: utility for prediction, *Chemical reviews*  
613 110 (2010) 5714–5789.
- 614 [30] T. Le, V. C. Epa, F. R. Burden, D. A. Winkler, Quantitative structure-  
615 property relationship modeling of diverse materials properties, *Chemical  
616 reviews* 112 (2012) 2889–2919.
- 617 [31] M. E. Erickson, M. Ngongang, B. Rasulev, A refractive index study of  
618 a diverse set of polymeric materials by QSPR with quantum-chemical  
619 and additive descriptors, *Molecules* 25 (2020).
- 620 [32] S. A. Schustik, F. Cravero, I. Ponzoni, M. F. Daz, Polymer informatics:  
621 Expert-in-the-loop in QSPR modeling of refractive index, *Computa-  
622 tional Materials Science* 194 (2021) 110460.
- 623 [33] A. J. Holder, L. Ye, J. D. Eick, C. C. Chappelow, A quantum-mechanical  
624 QSAR model to predict the refractive index of polymer matrices, *QSAR  
625 & Combinatorial Science* 25 (2006) 905–911.
- 626 [34] P. R. Duchowicz, S. E. Fioressi, D. E. Bacelo, L. M. Saavedra, A. P.  
627 Toropova, A. A. Toropov, QSPR studies on refractive indices of struc-  
628 turally heterogeneous polymers, *Chemometrics and Intelligent Labora-  
629 tory Systems* 140 (2015) 86–91.

- [35] F. Jabeen, M. Chen, B. Rasulev, M. Ossowski, P. Boudjouk, Refractive indices of diverse data set of polymers: A computational QSPR based study, *Computational Materials Science* 137 (2017) 215–224.
- [36] A. G. Mercader, P. R. Duchowicz, Encoding alternatives for the prediction of polyacrylates glass transition temperature by quantitative structure–property relationships, *Materials Chemistry and Physics* 172 (2016) 158–164.
- [37] A. G. Mercader, D. E. Bacelo, P. R. Duchowicz, Different encoding alternatives for the prediction of halogenated polymers glass transition temperature by quantitative structure–property relationships, *International Journal of Polymer Analysis and Characterization* (2017) 1–10.
- [38] A. Karuth, A. Alesadi, W. Xia, B. Rasulev, Predicting glass transition of amorphous polymers by application of cheminformatics and molecular dynamics simulations, *Polymer* 218 (2021) 123495.
- [39] A. Toropov, A. Toropova, V. Kudyshkin, N. Bozorov, S. Rashidova, Applying the monte carlo technique to build up models of glass transition temperatures of diverse polymers, *Structural Chemistry* 31 (2020) 1739–1743.
- [40] F. Cravero, M. J. Martnez, I. Ponzoni, M. F. Daz, Computational modelling of mechanical properties for new polymeric materials with high molecular weight, *Chemometrics and Intelligent Laboratory Systems* 193 (2019) 103851.
- [41] F. Cravero, M. J. Martnez, G. Vazquez, M. F. Daz, I. Ponzoni, Feature learning applied to the estimation of tensile strength at break in polymeric material design, *Journal of Integrative Bioinformatics* 13 (2016) 15–29.
- [42] T. Zhu, Y. Jiang, C. Haomiao, R. P. Singh, B. Yan, Development of pp-LFER and QSPR models for predicting the diffusion coefficients of hydrophobic organic compounds in ldpe, *Ecotoxicology and Environmental Safety* 190 (2020) 110179.
- [43] M. Li, H. Yu, Y. Wang, J. Li, G. Ma, X. Wei, QSPR models for predicting the adsorption capacity for microplastics of polyethylene, polypropylene and polystyrene, *Scientific Reports* 10 (2020) 14597.

- 663 [44] N. Villanueva, B. Flaconnèche, B. Creton, Prediction of alternative  
664 gasoline sorption in a semicrystalline poly(ethylene), *ACS combinatorial*  
665 *science* 17 (2015) 631–640.
- 666 [45] L. Starck, L. Pidol, N. Jeuland, T. Chapus, P. Bogers, J. Bauldreay,  
667 Production of hydroprocessed esters and fatty acids (HEFA) - optimisa-  
668 tion of process yield, *Oil Gas Sci. Technol. - Rev. IFP Energies nouvelles*  
669 71 (2016) 10.
- 670 [46] C. Hall, B. Rauch, U. Bauder, P. Le Clercq, M. Aigner, Predictive ca-  
671 pability assessment of probabilistic machine learning models for density  
672 prediction of conventional and synthetic jet fuels, *Energy & Fuels* 35  
673 (2021) 2520–2530.
- 674 [47] B. Creton, Chemoinformatics at IFP energies nouvelles: Applications in  
675 the fields of energy, transport, and environment, *Molecular Informatics*  
676 36 (2017) 1700028.
- 677 [48] C. Nieto-Draghi, G. Fayet, B. Creton, X. Rozanska, P. Rotureau, J.-  
678 C. de Hemptinne, P. Ungerer, B. Rousseau, C. Adamo, A general  
679 guidebook for the theoretical prediction of physicochemical properties of  
680 chemicals for regulatory purposes, *Chemical Reviews* 115 (2015) 13093–  
681 13164.
- 682 [49] P. Gramatica, Principles of QSAR models validation: Internal and ex-  
683 ternal, *QSAR and Combinatorial Science* 26 (2007) 694–701.
- 684 [50] E. N. Muratov, E. V. Varlamova, A. G. Artemenko, P. G. Polishchuk,  
685 V. E. Kuz’Min, Existing and developing approaches for QSAR analysis  
686 of mixtures, *Molecular Informatics* 31 (2012) 202–221.
- 687 [51] T.-B. Nguyen, J.-C. de Hemptinne, B. Creton, G. M. Kontogeorgis,  
688 Characterization scheme for property prediction of fluid fractions origi-  
689 nating from biomass, *Energy & Fuels* 29 (2015) 7230–7241.
- 690 [52] D. Steinmetz, K. R. Arriola Gonzalez, R. Lugo, J. Verstraete, V. Lachet,  
691 A. Mouret, B. Creton, C. Nieto-Draghi, Experimental and mesoscopic  
692 modeling study of water/crude oil interfacial tension, *Energy & Fuels*  
693 (2021).

- [53] C. Vendevre, R. Ruiz-Guerrero, F. Bertoncini, L. Duval, D. Thiébaut, Comprehensive two-dimensional gas chromatography for detailed characterisation of petroleum products, *Oil Gas Sci. Technol. - Rev. IFP Energies nouvelles* 62 (2007) 43–55.
- [54] SMARTS - a language for describing molecular patterns; daylight chemical information systems inc.: Laguna niguel, ca, Accessed in 2020. URL: <http://www.daylight.com/dayhtml/doc/theory/theory.smarts.html>.
- [55] RDKit: Open-Source Cheminformatics Software, Accessed in 2020. URL: <http://www.rdkit.org/>.
- [56] C. Muller, A. G. Maldonado, A. Varnek, B. Creton, Prediction of optimal salinities for surfactant formulations using a quantitative structure-property relationships approach, *Energy Fuels* 29 (2015) 4281–4288.
- [57] D. Searson, D. Leahy, M. Willis, GPTIPS: an open source genetic programming toolbox for multigene symbolic regression, *Proceedings of the International MultiConference of Engineers and Computer Scientists 2010 (IMECS 2010)*, Hong Kong, 17-19 March (2010) 77–80.
- [58] A. Gandomi, A. Alavi, C. Ryan, *Handbook of Genetic Programming Applications*, Springer International Publishing, New York, 2015.
- [59] D. Searson, *Handbook of Genetic Programming Applications*, in: [58], 2015.
- [60] B. Creton, I. Lévêque, F. Oukhemanou, Equivalent alkane carbon number of crude oils: A predictive model based on machine learning, *Oil Gas Sci. Technol. - Rev. IFP Energies nouvelles* 74 (2019) 30.
- [61] O. Agwu, J. U. Akpabio, A. Dosunmu, Modeling the downhole density of drilling muds using multigene genetic programming, *Upstream Oil and Gas Technology* (2021) 100030.
- [62] P. Gantzer, B. Creton, C. Nieto-Draghi, Inverse-QSPR for de novo design: A review, *Molecular Informatics* 39 (2020) 1900087.
- [63] P. Gantzer, B. Creton, C. Nieto-Draghi, Comparisons of molecular structure generation methods based on fragment assemblies and genetic graphs, *Journal of Chemical Information and Modeling* 61 (2021) 4245–4258.

- <sup>726</sup> [64] K. Sattari, Y. Xie, J. Lin, Data-driven algorithms for inverse design of  
<sup>727</sup> polymers, *Soft Matter* 17 (2021) 7607–7622.